SHP-1 that in turn functions to inactivate the kinase and negatively regulate TCR signal transduction. Therefore, the kinase is directly responsible for its own negative regulation.

REFERENCES AND NOTES

1. L. Howe and A. Weiss, *Trends Biochem. Sci.* **20**, 59 (1995).
2. J. G. Cyster and C. C. Goodnow, *Immunity* **2**, 13 (1995).
3. D. D'Ambrosio *et al.*, *Science* **268**, 293 (1995); G. Doody *et al.*, *ibid.* **269**, 242 (1995).
4. U. Klingmüller, U. Lorenz, L. Cantley, B. Neel, H. Lodish, *Cell* **80**, 729 (1995); T. Yi, J. Zhang, O. Miura, J. Ihle, *Blood* **85**, 87 (1995); T. Yi, A. L.-F. Mui, G. Krystal, J. N. Ihle, *Mol. Cell. Biol.* **13**, 7577 (1993).
5. D. R. Plas, R. J. Matthews, G. Roy, A. C. Chan, M. L. Thomas, unpublished data.
6. For transient transfection of Jurkat cells, equal amounts of pIL-2 luciferase and either pSFFV (empty vector), pSFFV–SHP-1, or pSFFV-SHP-1(C453S) were used. After 40 hours, cells were stimulated with PMA (500 ng/ml, Sigma), anti-TCR (antibody C305, 2 μg/ml), or a combination of PMA and anti-TCR, or a combination of PMA and 1 μM ionomycin (Calbiochem). After 6 hours of stimulation, the cells were harvested and lysates were used in a luciferase assay, according to the manufacturer's recommendations (Promega). For stable expression of dominant negative SHP-1(C453S) in Jurkat cells, cells were transfected with either pSFFV or pSFFV–SHP-1(C453S) in which the cDNA was appended at the 3′ end with a sequence encoding an epitope tag derived from c-*myc*. Cells were selected for G418 resistance. The resulting cell lines were cloned by limiting dilution, and individual clones were examined for the expression of SHP-1(C453S) by immunoblotting for the epitope tag. Cell lines were examined for equal expression of the TCR. Individual clones were stimulated with anti-TCR (2 μg/ml) for 0, 3, and 7 min and lysed in ice-cold lysis buffer [1% NP-40, 10 mM tris (pH 8.0), 150 mM NaCl, 1 mM phenylmethylsulfonyl fluoride (PMSF), 2 mM leupeptin, 3 mM pepstatin A, 5 mM EDTA, 0.4 mM $NaVO_3$, and 10 mM NaF]. Cell lysates for equal numbers of cells were separated on 8% SDS-polyacrylamide gel and immunoblotted with anti-phosphotyrosine (antibody 4G10, UBI). J.SHP-1 C/S 213 and J.neo are representative clones. 3L2 cells overexpressing SHP-1 or SHP-1(C453S), or vector control cell lines, were generated by transfection of cells with either cytomegalovirus–driven expression vector (BCMG) containing SHP-1 or SHP-1(C453S) cDNA, or vector with no insert. Neomycin-resistant cell lines were obtained, then individual clones were obtained by limiting dilution. Three individual clones were examined for each line. Equivalent expression of CD3 on the resulting clones was determined by flow cytometric analysis. 3L2 hybridoma cells were stimulated for 24 hours with the hemoglobin β peptide(64–76) with CH27 cells used as antigen-presenting cells.
7. B. D. Evavold, S. G. Williams, B. L. Hsu, S, Buus, P. M. Allen, *J. Immunol.* **148**, 3471 (1992).
8. U. Dechert *et al.*, *Eur. J. Biochem.* **231**, 673 (1995); D. Pei, B. G. Neel, C. T. Walsh, *Proc. Natl. Acad. Sci. U.S.A.* **90**, 1092 (1993).
9. G. Roy, J. Matthews, T. Woodford-Thomas, M. L. Thomas, *Adv. Protein Phosphatases* **9**, 121 (1995).
10. D. Pei, U. Lorenz, U. Klingmüller, B. G. Neel, C. T. Walsh, *Biochemistry* **33**, 15483 (1994).
11. R. Townley, S.-H. Shen, D. Banville, C. Ramachandran, *ibid.* **32**, 13414 (1993).
12. T. Yi and J. N. Ihle, *Mol. Cell. Biol.* **13**, 3350 (1993).
13. M. Campbell and N. Klinman, *Eur. J. Immunol.* **25**, 1573 (1995).
14. HeLa cells were infected with recombinant vaccinia virus encoding the T7 RNA polymerase. cDNAs in pBluescript (Stratagene) behind the T7 promoter for G-ζ, ZAP-70, SHP-1, SHP-1(C453S), and $p59^{fyn}$ were transfected into HeLa cells. Cells were lysed in 1% NP-40, 10 mM tris (pH 8.0), 150 mM NaCl, aprotinin (50 μg/ml), 2 mM leupeptin, 1 mM PMSF, and 5 mM iodoacetamide, and immunoprecipitation was then performed with specific antiserum. Immunoblotting was performed with 4G10 (anti-phosphotyrosine) and 2f3.2 (anti–ZAP-70) obtained from UBI. For kinase assays, $p59^{fyn}$ immunoprecipitates were incubated at 25°C for 5 min in 10 mM tris (pH 7.4), 10 mM $MgCl_2$, 10 mM $MnCl_2$, and 10 μCi [γ-P^{32}]adenosine triphosphate (ATP). Plaque-purified and titered baculovirus stocks were used to infect Sf9 cells at 5×10^6 plaque-forming units (pfu) per milliliter. For co-infections, viruses encoding either the GST–ZAP-70 fusion protein (GST–ZAP-70) or $p56^{lck}$ kinase domain were infected at a ratio of 9:1; for infections containing viruses encoding either GST–ZAP-70, $p56^{lck}$ kinase domain, or SHP-1 the ratio was 9:1:2. Cells were also infected with viruses encoding ZAP-70 and SHP-1. Results similar to infection with virus encoding ZAP-70 alone were observed. This is likely because of the requirement of an exogenous kinase to active ZAP-70. Cells were lysed in lysis buffer. ZAP-70 was purified on glutathione agarose (Sigma) according to the manufacturer's recommendations. For kinase assays, ZAP-70 bound to glutathione agarose was incubated at 25°C for 5 min in 10 mM tris (pH 7.4), 10 mM $MgCl_2$, 10 mM $MnCl_2$, and 10 μCi [γ-P^{32}]ATP, with Band III as an exogenous substrate.
15. Jurkat cells were stimulated with anti-TCR (2 μg/ml) for 2 min at 37°C or with 5 mM pervanadate for 10 min at room temperature. Cells were lysed, immunoprecipitated with anti–SHP-1, and analyzed by immunoblot for either SHP-1, ZAP-70, or phosphotyrosine as described. For binding with GST–SHP-1 fusion proteins, Jurkat cells were stimulated with pervanadate as described above or peroxide alone as a control and lysed in 1% brij containing 20 mM tris (pH 7.4), 140 mM NaCl, 5 mM EDTA, 1 mM PMSF, 2 mM leupeptin, aprotinin (20 μg/ml), and 5 mM iodoacetamide. Equal amounts of either GST, GST–SHP-1 SH2 domains (amino acids 1 to 222), or GST–SHP-1 catalytically inactive phosphatase domain (amino acids 237 to 595, C453S) were incubated with lysates from stimulated or unstimulated cells for 1 hour at 4°C and bound to glutathione agarose and Beads were collected by centrifugation and washed three times in brij lysis buffer, and samples were subjected to immunoblot analysis with anti–ZAP-70 (UBI).
16. H. Sun, C. H. Charles, L. F. Lau, N. K. Tonks, *Cell* **75**, 487 (1993); J. B. Bliska, J. C. Clemens, J. E. Dixon, S. Falkow, *J. Exp. Med.* **176**, 1625 (1992).
17. SHP-1 was produced in Sf9 cells and purified by affinity chromatography. A fusion protein of GST–ZAP-70 was produced in Sf9 cells in the presence or absence of $p56^{lck}$ kinase domain as described and purified on glutathione agarose in the presence of 5 mM iodoacetamide. Seven picomoles of ZAP-70 was mixed with 1.75 pmol of SHP-1 in 2 mM *p*-nitrophenylphosphate, 50 mM Hepes (pH 7.0), 5 mM EDTA, and 10 mM dithiothreitol for 1 hour at 37°C, and the amount of *p*-nitrophenylate was determined by measuring absorbance at 405 nm. Phosphatase activity in preparations of ZAP-70 and phosphorylated ZAP-70 was negligible. The fold increase in activity was determined by comparing it with the activity of SHP-1 alone. Background phosphatase activity was subtracted from the calculation.
18. R. J. Matthews, D. B. Borne, E. Flores, M. L. Thomas, *Mol. Cell. Biol.* **12**, 2396 (1992); R. C. Fuhlbrigge, S. M. Fine, E. R. Unanue, D. D. Chaplin, *Proc. Natl. Acad. Sci. U.S.A.* **85**, 5649 (1988).
19. E. D. C. McFarland and M. L. Thomas, *J. Biol. Chem.* **270**, 28103 (1995).
20. A. Chan *et al.*, *EMBO J.* **14**, 2499 (1995).

21. We thank P. Allen and A. Shaw for advice and the gifts of reagents, and L. Dustin, M. Tsotsiashvili, and T. Woodford-Thomas for reading the manuscript. A.C.C. is supported in part by the Arthritis Foundation and the Pews Scholars Program. D.R.P. is funded by the Lucille P. Markey Program. A.C.C. and M.L.T. are investigators at the Howard Hughes Medical Institute.

2 February 1996; accepted 22 April 1996

Entorhinal-Hippocampal Interactions Revealed by Real-Time Imaging

Toshio Iijima,* Menno P. Witter, Michinori Ichikawa, Takashi Tominaga, Riichi Kajiwara, Gen Matsumoto

The entorhinal cortex provides the major cortical input to the hippocampus, and both structures have been implicated in memory processes. The dynamics of neuronal circuits in the entorhinal-hippocampal system were studied in slices by optical imaging with high spatial and temporal resolution. Reverberation of neural activity was detected in the entorhinal cortex and was more prominent when the inhibition due to γ-aminobutyric acid was slightly suppressed. Neural activity was transferred in a frequency-dependent way from the entorhinal cortex to the hippocampus. The entorhinal neuronal circuit could contribute to memory processes by holding information and selectively gating the entry of information into the hippocampus.

A number of mechanisms have been proposed to underlie memory formation in the central nervous system, including long-lasting changes in synaptic efficacy (*1*) and reverberation of activity in a closed loop of excitatory neurons (*2*) as demonstrated in the cerebellonuclear-pontonuclear system (*3*). In the entorhinal-hippocampal system, both mechanisms have been proposed to underlie the significant contribution of this system to learning and memory (*4*). The hippocampus (*5*) is a crucial structure for memory processes, and the closely associated entorhinal cortex (EC) likely executes a specific role as well (*6*). Superficial layers of the EC receive sensory inputs from parts of

T. Iijima, M. Ichikawa, T. Tominaga, G. Matsumoto, Molecular and Cellular Neuroscience Section, Electrotechnical Laboratory, 1-1-4 Umezono, Tsukuba, Ibaraki 305, Japan.
M. P. Witter, Graduate School for Neuroscience, Research Institute Neuroscience, Vrije Universiteit, Department of Anatomy and Embryology, Van der Boechorststraat 7, 1081 BT Amsterdam, Netherlands.
R. Kajiwara, Information Science, Tohoku University, Sendai 980, Japan.

*To whom correspondence should be addressed.

the association cortex and convey that information to the hippocampus. The output of the hippocampus is subsequently returned to the deep layers of EC, which may return the information either to the association cortex, where the long-term storage of information takes place (6), or to the superficial layers of EC (7).

Within a horizontal slice preparation,

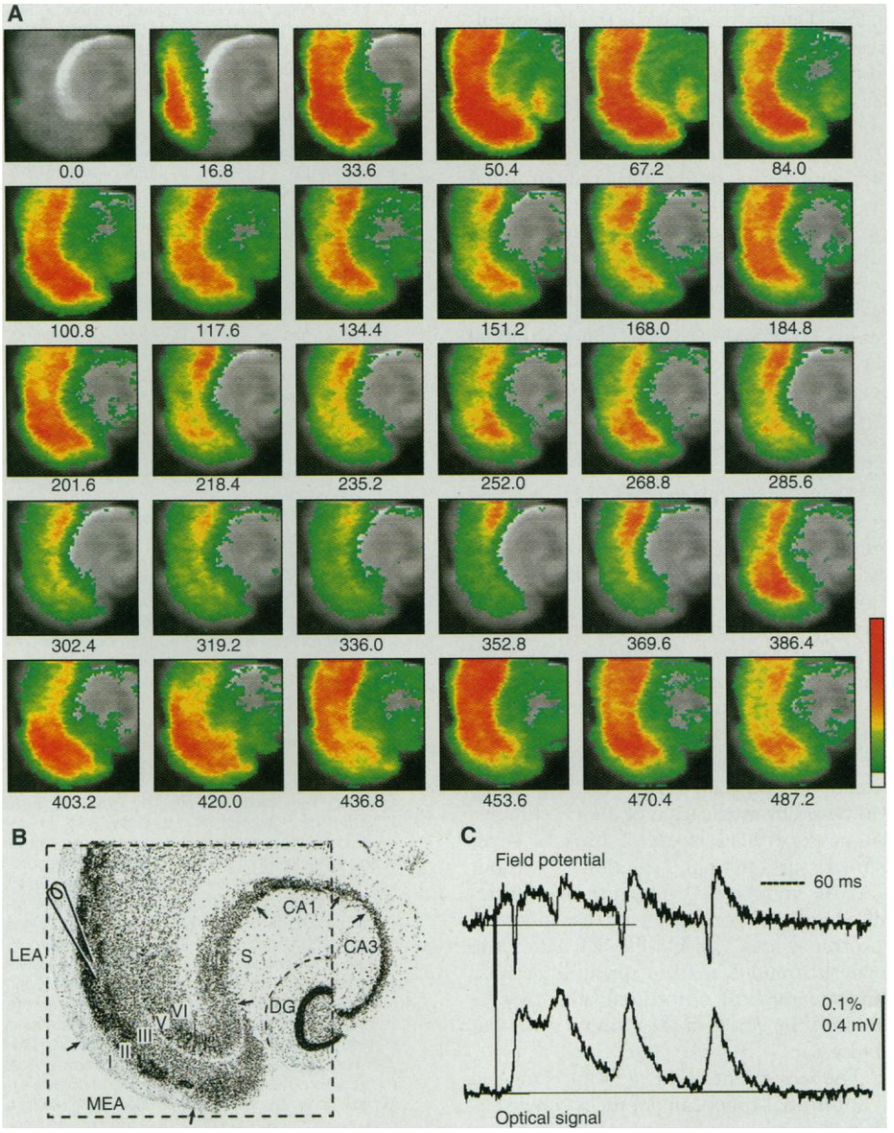

Fig. 1. (**A**) Real-time imaging of the spread of neural activity in the entorhinal-hippocampal slice (*9*) with 5 μM bicuculline added to the medium. The time after the stimulation is indicated below each image (in milliseconds). Optical recording with fluorescence voltage-sensitive dye (*10*) was made from the square area in (B), which included EC and the hippocampus. The stimulating electrode was placed between layers II and III. At 1.2 ms after stimulation, a spot of about 200 μm in diameter was activated, the activity of which expanded to a strip of about 1.4 mm by 0.7 mm in the superficial layer in 4.8 ms (not shown). Neural activity was encoded as pseudocolor and superimposed on the bright-field images. The length of the color code bar corresponds to a 0.1% fractional change in fluorescence signal. A fraction of each optical signal, the amplitude of which was below the maximum amplitude of background noise, was not color coded. Reverberation was observed only in horizontal slices obtained from the ventral part of the rat brains, 2.4. to 3.0 mm dorsal to the interaural plane. (**B**) Digitized image of the counterstained slice in (A) (*11*). Abbreviations: DG, dentate gyrus; LEA, lateral entorhinal area; MEA, medial entorhinal area; and S, subiculum. (**C**) An optical signal (lower trace) recorded by a pixel over a part of MEA is compared to the field potential (upper trace) obtained from the same site simultaneously. The record was obtained from a slice other than the one shown in (A) and (B), but under similar conditions. (**Supplement**) Reverberation of neural activity in EC and transfer of activity from EC to the hippocampus. The movie is available on *Science* On-Line (*14*).

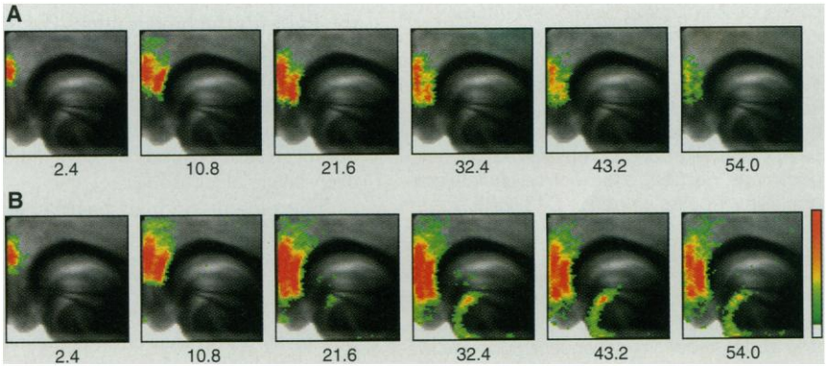

Fig. 2. Real-time imaging of neuronal activity in the entorhinal-hippocampal slice (*9*) superfused with normal solution. Optical recording was made with the use of absorption dye (*10*). Repetitive stimulation (1 Hz) was applied to the LEA at a position comparable to that illustrated in Fig. 1B. (**A**) Propagation of activity after the first stimulus is restricted to superficial and deep layers of LEA, with only minor spread into MEA. (**B**) Propagation of activity after the seventh stimulus. After 21.6 ms, activation enters the dentate gyrus, subsequently spreading along its transverse extent (32.4 ms). Activity was almost stable up to 60 ms, after which a decline occurred. Even after the second stimulus, the medial spread of activity in EC was evident. The second through fifth stimuli also resulted in weak and restricted activation of the dentate gyrus. Only after the sixth and seventh stimuli was activation apparent in the dentate gyrus along its transverse extent . The length of the color code bar corresponds to a 0.05% fractional change. (**Supplement**) Gating the entry of neural activity into the hippocampus, the movie is available on *Science* On-Line (*14*).

large portions of the entorhinal-hippocampal circuit are conserved (8). To reveal the functional dynamics of this circuitry, we visualized the propagation of neural activity in slices (9) that followed entorhinal stimulation through the use of voltage-sensitive dyes and real-time optical imaging (*10*, *11*). Because the propagation of neural activity in a slice can be suppressed by local inhibitory neurotransmission, we performed some of the optical recordings in slices bathed in bicuculline (1 or 5 μM) to partly suppress the inhibition by γ-aminobutyric acid (GABA)–containing inhibitory neurons.

Figure 1 shows the optical imaging of the propagation of neural activities in a horizontal slice of the rat brain containing the EC and hippocampus (*12*). Before stimulation, no spontaneous activity was recorded by optical imaging. Focal neural excitation in two of the superficial layers (layers II and III) of EC was evoked by a single electrical stimulation (Fig. 1B). The activity first spread laterally and medially in the superficial layers and subsequently led to activation of the deep layers (layers V and VI). At 33.6 ms after EC stimulation, activity invaded the hippocampus.

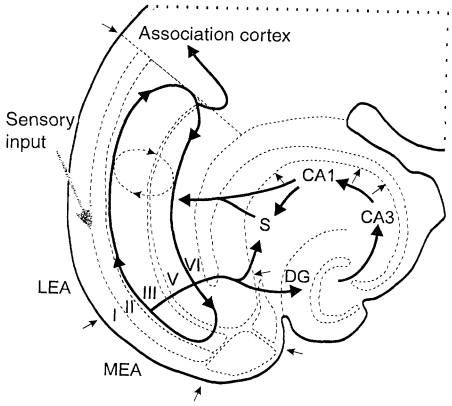

Fig. 3. Model of neural circuits that may underlie the propagation of neural activity in EC and the hippocampus. The EC contains a closed neuronal loop, including variable transverse and radial local connections (*19*). One of the possible local circuits corresponding to the activation patterns in Fig. 1 is indicated by the solid line. Input-output pathways link this network to the hippocampus and the association cortex. Incoming sensory information from adjacent association areas (gray arrow) influences the superficial layers of EC. By the perforant path, this activity could be transferred to the hippocampus. Resulting activity of the dentate granular cells will be transferred to CA3, CA1, and the subiculum. In parallel, the incoming activity may be held in the entorhinal reverberating circuit. Eventually, processed information will enter the entorhinal network (*7*). Over time, the repetitive activation of the superficial and deep layers of EC may lead to frequency-dependent multiple activations of the hippocampal formation; alternatively, the EC could convey information to the association cortex.

Although activity of the hippocampus disappeared around 151.2 ms after the stimulation, EC remained active. During the next 200 ms, the activity reverberated at least twice along the medial-to-lateral axis of EC. During this period, the hippocampus showed only partial and weak activation. The next excitation of EC, which began at 352.8 ms, again induced activation of the hippocampus. The excitation that appeared laterally in the deep layers of EC moved medially, and at about 386.4 ms, transfer to the superficial layers occurred. Subsequently, activity entered the hippocampus and remained present for about 70 ms. During that same period, activity reverberated once more in EC and ceased after 500 ms (*13*). This pattern of activation can be viewed in real time in *Science* On-Line (*14*). Based on calculations from these data, the conduction velocity in each layer ranges from 0.04 to 0.09 m/s (*15*).

A single stimulus applied to EC resulted in several reverberatory waves in EC. In only two of the reverberations, activity invaded the hippocampus. Neurons in the superficial layers of EC, which send their axons to the hippocampus, are under strong local inhibitory control, which can be overcome by higher frequency stimulation (*16*). It is possible that reverberation leads to repetitive stimulation, which overcomes the inhibitory component that is still present in the slice (*17*). This hypothesis was tested by application of a 1-Hz stimulus to the superficial layers of LEA of slices bathed in normal solution (without $GABA_A$ antagonists). The first stimulus resulted only in restricted activation in lateral entorhinal area (LEA) (Fig. 2). After the seventh stimulus, marked spread of activity into the medical entorhinal area (MEA) and into the whole of the dentate gyrus was observed.

The movement of the activity as imaged in entorhinal-hippocampal slices can be explained by the interaction of at least two circuits, one constituting a reverberating entorhinal circuit and the other connecting the EC with the hippocampus (Fig. 3). The reverberating circuit is driven not only by activation of the superficial layers, which are the major recipients of multimodal sensory inputs (*7*), but also by hippocampal output from CA1 and the subiculum to the deep layers of EC (*18*).

The present findings have at least two functional implications. First, the presence of reverberating circuits indicates that EC may hold information for a certain period of time. Second, by selectively gating information flow, entorhinal circuits may subserve spatial and temporal integration of entorhinal activity before information is conveyed to the hippocampus.

REFERENCES AND NOTES

1. T. V. P. Bliss and G. L. Collingridge, *Nature* **361**, 31 (1993); R. Malinow, *Science* **266**, 1195 (1994); B. L. McNaughton and R. G. M. Morris, *Trends. Neurosci.* **10**, 408 (1987).
2. G. M. Edelman, *The Remembered Present: A Biological Theory of Consciousness* (Basic Books, New York, 1989); S. A. Deadwyler, J. R. West, C. W. Cotman, G. Lynch, *Exp. Neurol.* **49**, 35 (1975); D. O. Hebb, *The Organization of Behavior* (Wiley, New York, 1949).
3. N. Tsukahara, *Brain Res.* **40**, 67 (1972).
4. W. B. Scoville and B. J. Milner, *J. Neurol. Neurosurg. Psychiatry* **20**, 11 (1957); M. Mishkin, *Nature* **273**, 297 (1978); S. Zola-Morgan and L. R. Squire, *Behav. Neurosci.* **100**, 155 (1986); L. E. Jarrard, *Behav. Neural Biol.* **60**, 9 (1993).
5. The term hippocampus comprises the dentate gyrus, Ammon's horn or hippocampus proper, and the subiculum.
6. L. R. Squire and S. Zola-Morgan, *Science* **253**, 1380 (1991); S. Zola-Morgan, L. R. Squire, S. J. Ramus, *Hippocampus* **4**, 483 (1994); H. Eichenbaum, T. Otto, N. J. Cohen, *Behav. Brain Sci.* **17**, 449 (1994).
7. G. W. Van Hoesen, *Trends Neurosci.* **5**, 345 (1982); M. P. Witter, H. J. Groenewegen, F. H. Lopes da Silva, A. H. M. Lohman, *Progr. Neurobiol.* **33**, 161 (1989); R. S. G. Jones, *Trends Neurosci.* **16**, 58 (1993); J. J. Chrobak and G. Buzsaki, *J. Neurosci.* **14**, 6160 (1995).
8. The connections between the medial entorhinal cortex and the hippocampus are preserved [C. L. Boulton, D. V. Haebler, U. Heinemann, *Hippocampus* **2**, 99 (1992); M. P. Witter, *ibid.* **3** (suppl.), 33 (1993); R. S. G. Jones, *Trends Neurosci.* **16**, 58 (1993)].
9. Cortical slices about 400 μm thick were prepared from male Wistar rats (about 300 g). Slices including the hippocampus and the entorhinal cortex were prepared by serially sectioning the brain horizontally, starting from the ventral surface of the brain.
10. The slice was submerged in a chamber on the stage of an epifluorescence microscope and stained with the voltage-sensitive dye RH-795 (Molecular Probes) (0.5 mg/ml for 3 to 4 min) [A. Grinvald, R. D. Frostig, E. Lieke, R. Hildesheim, *Physiol. Rev.* **68**, 1285 (1988)]. The fluorescence associated with membrane potential changes was measured with a high-speed imaging photodetector. Some optical recordings were made with the absorption voltage-sensitive dye RH-155 (Molecular Probes). The optical recording methods with RH-155 were similar to those reported elsewhere (*15*) [T. Iijima, G. Matsumoto, Y. Kidokoro, *Neuroscience* **51**, 211 (1992)]. The results were similar for both fluorescence and absorption measurements, although the fluorescent dye always gave larger optical signals; the maximum fractional change in optical signal was about 0.15% with RH-795 and about 0.05% with RH-155. Each optical record was obtained in a single trial, and no averaging was done. The slice was activated by delivering a short current pulse of 300-μs duration through electrically polished thin tungsten wire. The superfusing solution contained 124 mM NaCl, 5 mM KCl, 2 mM $CaCl_2$, 1.25 mM $MgSO_4$, 1.25 mM NaH_2PO_4, 22 mM $NaHCO_3$, and 10 mM glucose (pH 7.4). The hardware and software for optical recording were developed in our laboratory [M. Ichikawa, T. Iijima, G. Matsumoto, *Brain Mechanisms of Perception and Memory*, T. Ono, L. R. Squire, M. E. Raichle, D. I. Perrett, M. Fukuda, Eds. (Oxford Univ. Press, New York, Oxford, 1993), pp. 638–648]. The photodetector was a MOS sensor composed of 128 by 128 elements and was directly interfaced to a microcomputer. To improve the signal-to-noise ratio, we averaged 2 by 2 pixel groups into a single element, and thus images are presented as 64 by 64 pixels. The photodetector imaged a slice area of about 4.2 mm by 4.2 mm; each element thus covered 65 μm^2. At this spatial resolution, we could image the structure of neural tissue as well as record neural activity. The optical recording system had a time resolution (frame rate) of 0.6 ms.
11. After recording, slices were fixed in 4% paraformaldehyde for 1 to 2 hours, then cryoprotected with dimethylsulfoxide (DMSO). Forty-μm-thick sections

were cut on a freezing microtome, mounted on glass slides from a 0.2% gelatin solution, and counterstained with cresyl violet. Sections were photographed and prints were digitized (Fig. 1B).
12. The changes in optical signal likely represent predominantly the electrical activity of neurons (synaptic potentials and spikes), because they coincide with field potentials recorded over the same area of the slice (Fig. 1C). The spatial resolution of the measurement is not sufficient to detect the behavior of individual neurons. Therefore, no inferences can be made concerning the neuronal properties of the underlying entorhinal network.
13. In this slice, inhibition was partly suppressed by 5 μM bicuculline. Comparable observations were obtained in 23 slices (out of 28 of horizontal slices obtained from the ventral part of the brain, 2.4 mm to 3.0 mm dorsal to the interaural plane) under similar conditions and in 26 slices (out of 31) with only 1 μM of bicuculline. Without bicuculline (n = 56), the number of reverberating cycles was always limited to one, generally without subsequent activation of the hippocampus. Bicuculline could have altered the stability of the preparation and resulted in epileptiform activity. However, we concluded that this was not the case because (i) no activity was recorded before stimulation to EC was applied; (ii) stimulation of EC evoked activity only for 600 ms, and no activity was measured afterward; (iii) no significant change in propagation patterns was seen during sessions (up to 2 hours); (iv) directly adjacent slices under similar conditions consistently did not show any oscillations; and (v) no overall oscillatory activity is seen in the hippocampus of the same slice [E. W. Lothman, E. H. Bertram III, J. L. Stringer, *Prog. Neurobiol.* **37**, 1 (1991); U. Heinemann *et al.*, *Epilepsy Res. Suppl.* **7**, 273 (1992).
14. The movie is available at http://science-mag.aaas.org/science/feature/beyond/#iijima.
15. I. Vranesic, T. Iijima, M. Ichikawa, G. Matsumoto, T. Knopfel, *Proc. Natl. Acad. Sci. U.S.A.* **91**, 13014 (1994).
16. R. S. G. Jones, *Trends Neurosci.* **16**, 58 (1993); *Hippocampus* **5**, 125 (1995); D. M. Finch, A. M. Tan, M. Isokawa-Akesson, *J. Neurosci.* **8**, 2213 (1988); D. M. Finch, E. E. Wong, E. L. Derian, T. L. Babb, *Brain Res.* **397**, 205 (1986). The frequency-dependent decline in GABA inhibition may be due to desensitization of GABA receptors, to changes in equilibrium potentials for Cl^- and K^+ resulting from redistributed ion gradients, or to the feedback inhibition of GABA release after activation of presynaptic $GABA_B$ or $GABA_A$ receptors or both [M. McCarren and B. E. Alger, *J. Neurophysiol.* **53**, 557 (1985); J. R. Huguenard and B. E. Alger, *ibid.* **56**, 1 (1986); S. M. Thompson and B. H. Gahwiler, *ibid.* **61**, 501 (1989); R. A. Deisz and D. A. Prince, *J. Physiol. (London)* **412**, 513 (1989); L. S. Benardo, *Brain Res.* **607**, 81 (1993)].
17. Even in the presence of bicuculline (1 to 5 μM), membrane depolarizations were generally followed by long-lasting hyperpolarizations, which implies that the inhibitory system is not fully suppressed. In normal solution, stimulus frequencies of 1 Hz and higher can overcome the local inhibition (*16*). Thus, with a partial suppression of inhibition, the reverberating circuit at 0.1 Hz might be sufficient to overcome inhibition, resulting in activation of the perforant pathway.
18. In similar preparations, stimulation of either CA3 or the subiculum led to activation of the deep layers of EC and subsequent reverberating activity. Also, direct stimulation laterally in the deep layers of LEA resulted in the spread of activity in the deep layers to MEA, subsequent spread into superficial layers of MEA, followed by activation of the reverberating circuit.
19. We thank D. G. Amaral, A. H. M. Lohman, F. H. Lopes da Silva, R. Malinow, and W. J. Wadman for their suggestions and discussion. M.P.W. was supported by a travel grant from the Agency of Industrial Science and Technology (AIST) of Japan and the Netherlands Organization for Scientific Research (NWO).

4 August 1995; accepted 14 March 1996

TAB1: An Activator of the TAK1 MAPKKK in TGF-β Signal Transduction

Hiroshi Shibuya, Kyoko Yamaguchi, Kyoko Shirakabe, Akane Tonegawa, Yukiko Gotoh, Naoto Ueno, Kenji Irie, Eisuke Nishida, Kunihiro Matsumoto*

Transforming growth factor–β (TGF-β) regulates many aspects of cellular function. A member of the mitogen-activated protein kinase kinase kinase (MAPKKK) family, TAK1, was previously identified as a mediator in the signaling pathway of TGF-β superfamily members. The yeast two-hybrid system has now revealed two human proteins, termed TAB1 and TAB2 (for TAK1 binding protein), that interact with TAK1. TAB1 and TAK1 were co-immunoprecipitated from mammalian cells. Overproduction of TAB1 enhanced activity of the plasminogen activator inhibitor 1 gene promoter, which is regulated by TGF-β, and increased the kinase activity of TAK1. TAB1 may function as an activator of the TAK1 MAPKKK in TGF-β signal transduction.

The mitogen-activated protein kinase (MAPK) pathway is a conserved eukaryotic signaling module that converts receptor signals into various outputs. This pathway includes three protein kinases: MAPKKK, MAPKK, and MAPK; MAPK is activated through phosphorylation by MAPKK, which is first activated by MAPKKK (*1*). A member of the MAPKKK family, TAK1 (TGF-β–activated kinase 1), that functions in the signaling pathway of TGF-β superfamily members has been identified (*2*). TGF-β signals through a heteromeric complex of type I and type II TGF-β receptors, which are transmembrane proteins that contain cytoplasmic serine- and threonine-specific kinase domains (*3*). However, little is known at the molecular level of the signaling mechanism downstream of the TGF-β receptors.

To analyze the TAK1-dependent pathway that functions in TGF-β signal transduction, we used the yeast two-hybrid system (*4*) to search for proteins that directly interact with TAK1. Yeast cells were co-transformed with a TAK1 expression vector, encoding the LexA DNA binding domain fused to TAK1 (*5*), and plasmids containing human brain cDNA expression library clones fused to DNA encoding the GAL4 activation domain (GAD). Twenty-six positive clones encoding two distinct proteins, named TAB1 and TAB2, were obtained from ~1×10^6 transformants. The GAD fusion proteins expressed by the two classes of library isolates will be referred to as GAD-TAB1 and GAD-TAB2. To localize the regions in TAK1 responsible for interaction with TAB1 and TAB2, we examined a set of LexA-TAK1 deletion chimeras in two-hybrid assays (Fig. 1A). These studies revealed that TAB1 and TAB2 interact with the NH_2- and COOH-terminal domains of TAK1, respectively.

Proteins that interact with TAK1 may include both upstream regulators and downstream targets. If either TAB1 or TAB2 has a role in the activation of TAK1, one would expect that co-expression with TAK1 would influence the activity of the latter in yeast. We developed an in vivo system for assaying mammalian MAPKKK activity in the yeast pheromone-induced MAPK pathway (*2*, *6*). An activated form of TAK1 (TAK1ΔN) is able to substitute for Ste11p MAPKKK activity (*7*). Expression of full-length TAK1, however, fails to rescue the *ste11*Δ mutation, suggesting that yeast cells do not possess an activator of TAK1 (*2*). With the use of the yeast MAPK pathway, both GAD-TAB1 and GAD-TAB2 constructs were tested for their ability to complement the *ste11*Δ mutation in the presence of TAK1. Co-expression of GAD-TAB1 with TAK1 rescued the Ste11p deficiency, whereas GAD-TAB2 had no effect (Fig. 1B). These results indicate that TAB1 augments the activity of TAK1.

To determine whether TAB1 increases TAK1 activity in yeast cells, we transformed cells expressing or not expressing

H. Shibuya, Faculty of Pharmaceutical Sciences, Hokkaido University, Sapporo 060, and Precursory Research for Embryonic Science and Technology, Research Development Corporation of Japan, Hikari-dai, Kyoto 619-02, Japan.
K. Yamaguchi, K. Irie, K. Matsumoto, Department of Molecular Biology, Faculty of Science, Nagoya University, Chikusa-ku, Nagoya 464-01, Japan.
K. Shirakabe, Y. Gotoh, E. Nishida, Department of Genetics and Molecular Biology, Institute for Virus Research, Kyoto University, Sakyo-ku, Kyoto 606-01, Japan.
A. Tonegawa and N. Ueno, Faculty of Pharmaceutical Sciences, Hokkaido University, Sapporo 060, Japan.

*To whom correspondence should be addressed. E-mail: g44177a@nucc.cc.nagoya-u.ac.jp